UC Berkeley
UC Berkeley Previously Published Works

Title
On-ratio PDMS bonding for multilayer microfluidic device fabrication

Permalink
https://escholarship.org/uc/item/24s9t3vs

Journal
Journal of Micromechanics and Microengineering, 29(10)

ISSN
0960-1317

Authors
Lai, Andre
Altemose, Nicolas
White, Jonathan A
et al.

Publication Date
2019-10-01

DOI
10.1088/1361-6439/ab341e

Copyright Information
This work is made available under the terms of a Creative Commons Attribution License, availalbe at https://creativecommons.org/licenses/by/4.0/

Peer reviewed

eScholarship.org Powered by the California Digital Library
University of California

24-June-2019 Revision

On-ratio PDMS bonding for multilayer microfluidic device fabrication

Andre Lai[1], Nicolas Altemose[1], Jonathan A. White[1], Aaron M. Streets[1,2,*]

ORCID
A. Lai 0000-0003-3233-3590
N. Altemose 0000-0002-7231-6026
J. White 0000-0002-7009-3332

[1]Department of Bioengineering, University of California, Berkeley, Berkeley, CA 94720
[2]Chan Zuckerberg Biohub, San Francisco, CA 94158

*corresponding author:
email: astreets@berkeley.edu
phone: 510-664-4952

Abstract

Integrated elastomeric valves, also referred to as Quake valves, enable precise control and manipulation of fluid within microfluidic devices. Fabrication of such valves requires bonding of multiple layers of the silicone polymer polydimethylsiloxane (PDMS). The conventional method for PDMS-PDMS bonding is to use varied ratios of base to crosslinking agent between layers, typically 20:1 and 5:1. This bonding technique, known as “off-ratio bonding,” provides strong, effective PDMS-PDMS bonding for multi-layer soft-lithography, but it can yield adverse PDMS material properties and can be wasteful of PDMS. Here we demonstrate the effectiveness of “on-ratio” PDMS bonding, in which both layers use a 10:1 base-to-crosslinker ratio, for multilayer soft lithography. We show the efficacy of this technique among common variants of PDMS: Sylgard 184, RTV 615, and Sylgard 182.

Keywords:
microfluidic valves; microfabrication; lab-on-chip; uTAS; PDMS bonding; soft lithography

1. Introduction

The integrated elastomeric valve is the transistor of microfluidic circuits. Its development has enabled a suite of fundamental microfluidic components, including logic gates [1], peristaltic pumps [1], active cell traps [2], microfluidic formulators [3], and button membranes for mechanical trapping of molecular interactions [4]. These components are used to construct integrated microfluidic devices, which have proven to be powerful research tools in quantitative biology. Applications of such devices include PCR [5], digital PCR [6], qPCR on chip [7], microfluidic bioreactors [8], high-throughput parallel analysis [9], protein crystallography [10] and

single-cell analysis [11,12]. A vital component of integrated elastomeric valve fabrication is multilayer soft lithography [13], a technique which involves bonding casted layers of polydimethylsiloxane (PDMS) containing control and flow channels. While many methodologies exist to bond multiple layers of PDMS, including oxygen plasma bonding [14], adhesive bonding [15,16], and corona discharge bonding [17], the most common method for multilayer soft-lithography is termed “off-ratio bonding.” This technique takes advantage of the fact that PDMS is a two-component elastomer consisting of a base, also known as potting compound, and a crosslinking agent. To perform off-ratio bonding, two layers of partially cured PDMS with varying base-to-crosslinker ratios are brought into contact (figure 1). Because each layer has an excess of one component (when compared to standard 10:1 ratios), a concentration gradient is created. This gradient is thought to drive the diffusive transport of reactive molecules across the bonding interface to irreversibly bond the two layers [13,18]. The primary advantage of off-ratio bonding over the aforementioned methodologies is that the bond is not permanent until thermal curing. This enables iterative adjustment of the layers to align control and flow channels on the two respective layers. With plasma and corona discharge, bonding occurs instantaneously when the layers are brought into contact. If the layers are misaligned, further manipulation to realign the layers cannot be performed. With adhesive bonding, repeated manipulation of the layers may unevenly distribute the adhesive or may inadvertently push adhesive into channels.

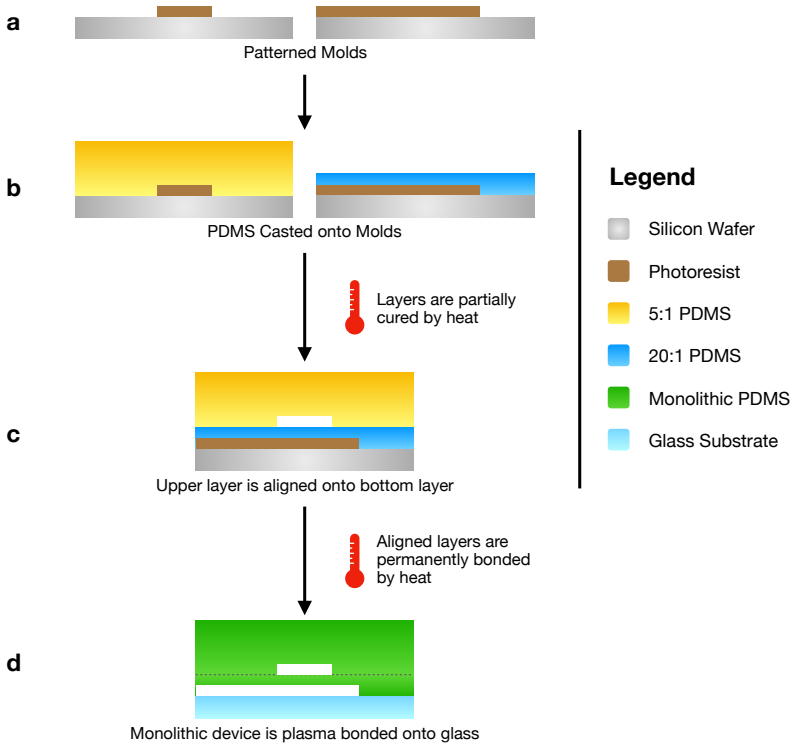

Figure 1. Multilayer soft-lithography using conventional off-ratio bonding. (a) Molds are patterned using photolithography. (b) 20:1 base-to-crosslinker PDMS is spin-coated onto the flow layer mold (left); 5:1 base-to-crosslinker PDMS is poured onto the control layer mold (right). (c) Each layer is partially thermally cured; the top layer is then aligned onto the bottom layer. (d) Permanent bonding between the aligned layers is achieved by a longer thermal curing step. The device is then plasma bonded onto a glass substrate

Off-ratio bonding provides a seamless and durable bond between the control and flow layers. This technique can hold up to 72 PSI (500 kPa) [19], well above a normal microfluidic operating range of 20 - 45 PSI (138 - 310 kPa). However, there are some drawbacks to using non-standard ratios of base to crosslinking agent. First, the two components of PDMS are typically manufactured and distributed for use with a 10:1 ratio of base to crosslinking agent. Because the thicker of the two layers often has the lower ratio, typically 5:1, unused base is accumulated and ultimately wasted. This can increase the cost per device by up to 100% when compared to devices fabricated using only 10:1 base-to-crosslinker ratios (see supplemental section S2). Second, the material properties of 5:1 and 20:1 PDMS differ from the properties of 10:1 PDMS, which is the specification given by the manufacturers. For many applications, augmented material properties may not affect device performance; likewise, physical material characteristics for 5:1 and 20:1 PDMS have been reported [20,21]. However, when layers of 5:1 and 20:1 PDMS are brought into contact for off-ratio bonding, the resulting material properties of the monolithic PDMS are poorly specified because diffusion of excess crosslinking agent across the bonding interface alters the base-to-crosslinker ratio of the final PDMS [22]. We have also observed differing optical properties when using non-standard ratios of PDMS (see supplemental figure S1). Lastly, a significant issue with off-ratio bonding is the potential toxicity of excess PDMS crosslinking agent with certain cell types [23]. PDMS with base-to-crosslinker ratios less than the conventional 10:1 ratio can cause certain cell types to detach and may inhibit them from reaching confluence [24].

Here we evaluate an alternative PDMS-PDMS bonding technique that helps mitigate the aforementioned issues associated with off-ratio bonding. We demonstrate that a stable and effective bond can be produced using a standard “on-ratio” mixture of 10:1 base to crosslinking agent for each layer. Previous studies have used on-ratio bonding in multilayer soft-lithography [25,26]; our study characterizes the performance of on-ratio bonding and presents a fabrication protocol with a variety of PDMS formulations. Successful on-ratio bonding operates on the same assumption as off-ratio bonding, which is that there are sufficient uncrosslinked chains and crosslinker molecules at the surface of each layer to catalyze inter-layer crosslinking. When layers are brought into contact and further cured, the surface monomers crosslink across the bond interface, resulting in the final monolithic device. We demonstrate the efficacy of this technique with the most commonly used PDMS formulations for soft lithography: Sylgard 184 and RTV 615. Effective on-ratio bonding relies on optimizing the partial curing step so that the thin and thick PDMS layers are robust enough to manipulate and align, yet under-cured enough to permit bonding. This trade-off results in a small window for partial curing of the thin layer. Therefore, we also tested a novel combination involving both Sylgard 184 and Sylgard 182. Sylgard 182 is physically and chemically similar to Sylgard 184; the primary difference is that Sylgard 182 takes longer to cure at room temperature. We tested Sylgard 182 on the premise that the longer cure time would better facilitate optimal partial curing of the thin layer. The thin layer cures much faster than the thick layer by nature of their respective thicknesses. By utilizing Sylgard 182 for the thin layer, while still using Sylgard 184 for the thick layer, the rate of partial curing for each layer was more manageable.

The bond integrities of the three PDMS formulations were compared to the those of devices using off-ratio bonding. When utilized to create microfluidic devices with integrated elastomeric valves, both on-ratio and off-ratio devices perform equally well within a normal microfluidic operating range of 20 - 45 PSI (138 - 310 kPa). We show that on-ratio bonding is a robust protocol that permits repeated manipulation of layers during alignment while eliminating disadvantages such as excess PDMS base, increased cost, equivocal material properties, and potentially limited biocompatibility.

2. Methods

2.1 Mold Fabrication

Molds were created using standard photolithography. In total, two control layer molds and one flow layer mold were fabricated. Photomasks were designed using AutoCAD and commercially produced using a 25400 dpi printer (CAD/Art Services, Inc., Bandon, Oregon). For the control layer molds, a dummy layer of SU8-2005 (MicroChem Corp., Westborough, MA) was spin-coated at 3500 rpm for 30 seconds onto 10 cm silicon wafers (University Wafer, Boston, MA) and subsequently cured to promote adhesion of the mold features. SU8-2025 Photoresist (MicroChem Corp., Westborough, MA) was then spin-coated on top of the dummy layer at 3500 rpm for 30 seconds to achieve a feature height of 25 μm. Exposure was performed using a UV Aligner (OAI, San Jose, CA). Specific baking temperatures, baking times, exposure dosages, and development times followed the MicroChem data sheet. For the flow layer mold, AZ-40XT-11d (Integrated Micro Materials, Argyle, TX) positive photoresist was spin coated at 3000 rpm for 30 seconds to achieve a feature height of 20 μm. Specific baking temperatures, baking times, and development times followed a previously published protocol [12]. To round the features, the wafer was baked on a hot plate for 1 min at 65°C, for 1 min at 95°C, and for 1 min 135°C to reflow the photoresist.

2.2 Device Fabrication

Soft-lithography procedures [27] were employed to fabricate each device. In order to test the bond interface, a thick control layer with microfluidic features was bonded to a thin dummy layer without microfluidic features (figure 2). In total, five device variants were fabricated: three device variants used on-ratio bonding and two device variants used off-ratio bonding. The PDMS composition of each layer in each device variant is detailed in Table 1. For each experiment, a total of 50 devices were fabricated (10 replicates per variant). Control molds and blank wafers (for the dummy layer) were first silanized with trichloromethlysilane (Sigma-Aldrich, St. Louis, MO) in a vacuum chamber for 20 min. This facilitated the removal of cured PDMS from the molds by passivating the silicon surface. Each PDMS variant was then mixed for 2 min with a vertical mixer and then degassed in a vacuum chamber. Sylgard variants (Dow Corning, Midland, MI) were degassed for 45 min and RTV 615 variants (Momentive Performance Materials, Inc., Waterford, NY) were degassed for 90 min. PDMS was then poured onto the control molds for a thickness of 0.4 cm and degassed for an additional 5 min. PDMS was spin-

coated onto the blank wafers. A two-step spin protocol was utilized. In the first step, PDMS was spun at 500 rpm, using an acceleration of 100 rpm/s and a 2 sec dwell time. In the second step, PDMS was spun to a final speed dependent on the PDMS variant and detailed in Table 1, using an acceleration of 500 rpm/s and a 60 sec dwell time. The second step spin speed was optimized for a thickness of 55 μm (see supplemental figure S2). The layers were then baked at 70°C using a forced air convection oven (Heratherm OMH60, Thermo Fisher Scientific, Waltham, MA) to partially cure the PDMS. Specific baking times for each layer are detailed in Table 1. After baking, the control layers were cut to size from the partially cured PDMS slab, inlet holes were punched using a precision punch (Accu-Punch MP10, Syneo, Angleton, TX; see supplemental section S1), and aligned onto the dummy layer. A final post-alignment baking step was performed at 70°C for 120 min to complete the bonding. The bonded devices were then mounted onto glass coverslips (VWR International, LLC, Radnor, PA) using oxygen plasma (Plasma Equipment Technical Services, Brentwood, CA), with five devices of the same variant on each coverslip. The other device designs, used to test pressure with large chamber geometries or to test valve responsivity, were fabricated according to the same protocol, with different master molds.

Table 1 PDMS Specifications, Baking Times, and Thin Layer Spin Speeds of Each Variant

Variant #	**Variant Composition**		**Baking Time at 70°C (min)**	**Spin Speed (rpm)**
1	Thick Layer	Sylgard 184 10:1	25	n/a
	Thin Layer	Sylgard 182 10:1	32	1400
2	Thick Layer	Sylgard 184 10:1	25	n/a
	Thin Layer	Sylgard 184 10:1	14	1400
3	Thick Layer	Sylgard 184 5:1	19	n/a
	Thin Layer	Sylgard 184 20:1	19	1900
4	Thick Layer	RTV 615 10:1	19	n/a
	Thin Layer	RTV 615 10:1	10	2000
5	Thick Layer	RTV 615 5:1	16	n/a
	Thin Layer	RTV 615 20:1	16	2000

2.2.1 Determining Pre-Alignment Partial Cure Baking Times

Partial cure baking times were determined by assessing bond performance and qualitative attributes of the PDMS itself. PDMS that was adequately partially cured was rigid enough for physical manipulation while tacky enough to create a sufficient bond. PDMS that was under-cured was too tacky on the surface. This resulted in difficulty with cutting, hole punching, and layer manipulation during alignment. Likewise, aligned layers often had excess air bubbles trapped between the layers, and channel collapse was more probable. Over-cured PDMS does not bond properly. Performing pressure tests on such devices resulted in the devices failing more frequently at lower pressures. We used the aforementioned qualities to determine a partial

cure baking time for each variant. Samples of each variant were baked until they matched the desired attributes. The “tacky-ness” of samples were assessed by gently placing a gloved finger in contact with the sample surface (see supplemental section S3). Samples were then bonded and subsequently tested.

2.2.2 Protocol Dependency on Oven

Soft-lithography fabrication protocols often utilize gravity convection ovens. The protocol reported here utilized a forced air convection oven. At any given temperature, we have found that a forced air convection oven will cure PDMS faster than a gravity convection oven. Thus, our protocol uses a reduced baking temperature of 70°C (compared to the more commonly used temperature of 80°C) to achieve more manageable baking times. A successful bond could still be achieved at 80°C in either a gravity or forced air convection oven, but baking times would have to be optimized in order to achieve a partial cure.

2.3 Experimental Set-Up

The pressure test experiments were conducted blind to avoid unintentional bias in the assessment of bond performance. Prior to connecting the pressure inlets to the devices, a neutral colleague unaffiliated with the experiment assigned each device an alphabetical code corresponding to which bonding variant was used. Following the end of each experiment, the codes were retrieved in order to process the results. To prepare the devices for experimental testing, a control channel in each device was filled with red dye (Fisher Science Education, Nazareth, PA) and pressurized to 20 PSI (138 kPa) (figure 2). The pressure delivered to each device was controlled by an independently addressable solenoid valve (Pneumadyne, Plymouth, MN). Each valve in this solenoid valve array was electronically actuated by the KATARA microfluidics controller and software [28]. See supplemental figure S3 for more information about the experimental set-up. A comprehensive description of the pneumatic infrastructure can be found in reference [29].

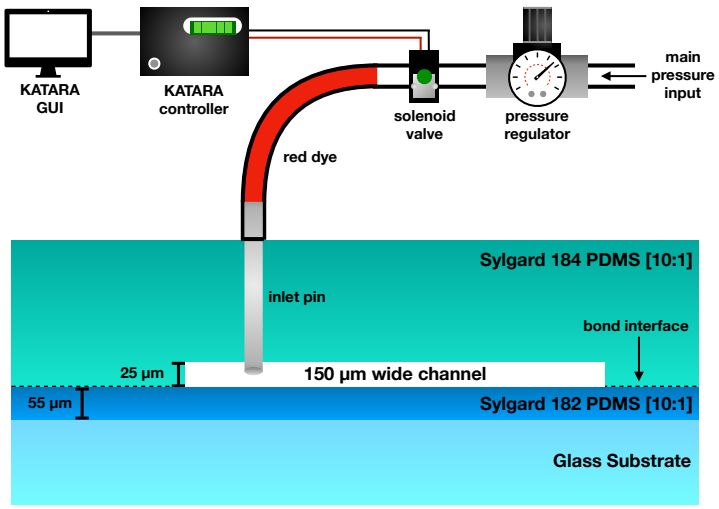

Figure 2. Schematic of experimental set-up: pressure from main pressure lines are controlled by a pressure regulator and actuated using a solenoid valve connected to the KATARA microcontroller and software GUI. Using this pressure, each device was filled with red dye to test the bond strength

2.4 Device Pressure Testing

All variants were tested in parallel. For each device, one microfluidic channel measuring 150 μm in width was pressurized at a steady pressure of 30 PSI (207 kPa) for 30 min. After 30 min at a constant 30 PSI, pressure was repeatedly actuated at 0.5 Hz for another 30 min to simulate valves opening and closing. This one-hour test was repeated at 45 PSI (310 kPa) and 60 PSI (414 kPa).

Qualitative examination of the red dye clearly showed whether or not delamination between the flow and control layers occurred, which is indicative of bond failure. During a delamination event, red dye escaped between the two layers. After a delamination event, red dye was no longer present in the clear tubing or in the microfluidic channels, and a path of delamination could be traced from the microfluidic channel to the device perimeter. In some cases, devices failed by other mechanisms not indicative of bond failure. These failure modes include splitting of the bulk PDMS or ejection of the inlet pin from the device itself (see supplemental figure S4) and are distinct from bond failure.

To further validate the bond strength of the devices that used on-ratio bonding, we performed experiments using devices with 7 mm diameter chamber geometries (see supplemental figure S3c). Previous studies have used large chambers to test bond strength in order to make the bond more susceptible to delamination [19]. With these large chambers, we could effectively test the bond strength of the devices to the point of failure without the need for pressure sources that could output higher pressures. These devices were set-up using the same procedure as described in methods section 2.3. They were tested using the same methodology described for the normal geometry devices, but without the 30 min of on/off actuation.

2.5 Valve Response Testing

While Sylgard 184 and RTV 615 are commonly used to fabricate valve-based microfluidic devices, the use of Sylgard 182 for such devices has not been reported. Thus, in order to validate valve performance with Sylgard 182, dynamic valve response testing was conducted. A more thorough study of valve response times is reported elsewhere [25]. The valves of devices fabricated using the 182/184 on-ratio bonding protocol were compared to valves of devices fabricated using the standard 184 off-ratio protocol. These devices were fabricated using the same set of molds; this ensured that channel geometry would not be a variable in valve responsivity. The PDMS thicknesses of the flow layers of each fabrication type were controlled to a height of 55 μm; this ensured that membrane thickness would not be a variable in valve responsivity. To test the opening and closing times of the valves, green dye (Fisher

Science Education, Nazareth, PA) was filled into a single flow channel, while water was dead-end filled into an overlapping control channel. The device was placed under a scanning confocal microscope (Olympus, Center Valley, PA). The valve was opened and closed under 20 PSI (138 kPa) of pressure repeatedly at 4 Hz. As the valve closes, green dye in the underlying channel is displaced (figure 3). When the valve returns to the open position, the green dye in the underlying channel is restored. Laser light was focused through the valve junction and a transmission detector recorded transmitted intensity during the series of valve actuations. The transmission intensity time series was then processed in R (R Foundation). Valve response times were calculated by determining the time required for the signal to transition between 10% and 90% of the maximum or minimum intensity.

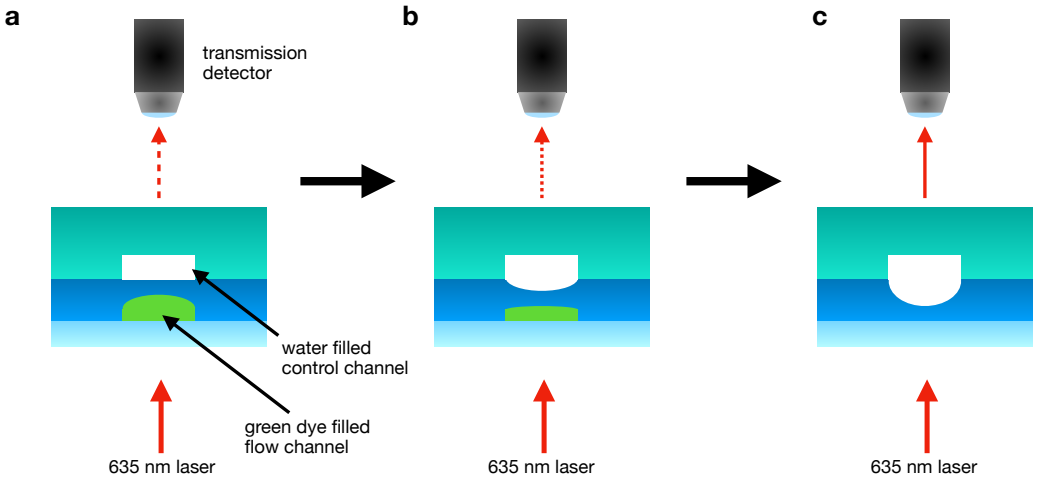

Figure 3. Schematic of valve responsivity measurement. (a) The valve is fully open. Green dye fills the lower flow channel, and water fills the upper control channel. Transmission is at a minimum. (b) The upper control channel is pressurized, and the valve is in the process of closing. The green dye is being displaced. Transmission is increasing. (c) The valve has fully closed the flow channel. All green dye has been displaced and transmission is at a maximum

3. Results and Discussion

On-ratio bonding relies on pre-baking the flow and control layers, leaving the PDMS only partially cured before aligning so that a final curing step can permanently bond the two layers. The temperature and curing time of this pre-bake step must be optimized so that the thick and thin PDMS layers are cured enough to manipulate and align, but under-cured enough to allow remaining crosslinking of unreacted species between the two layers for permanent bonding. This strategy is also used in off-ratio bonding; however, by creating an excess of crosslinker in one layer and a deficiency in the other, off-ratio bonding ensures that there will be unreacted species at the bonding interface. In on-ratio bonding there is less tolerance to over-baking the PDMS during the pre-bake step, which would compromise the integrity of the bond. Using a

forced air convection oven, we determined pre-bake times at 70ºC, for both the thick and thin layers (table 1) to achieve optimal partial curing and strong on-ratio bonding.

3.1 Bond Performance

In total, 100 devices were tested: 20 devices for each variant. When testing devices with standard channel geometry (150 μm width and 25 μm height) using typical control pressures (30-45 PSI), no delamination occurred, and all on-ratio variants performed equally to the off-ratio variants. At 60 PSI, 95% of the RTV did not delaminate while 75% of the 184/184 on-ratio devices did not delaminate (figure 4). None of the 182/184 on-ratio devices delaminated at 60 PSI. We suspect that 182/184 devices performed better due to Sylgard 182's longer cure time. The longer cure time translates to a reduced rate of curing, thus facilitating partial curing.

From figure 4, a "failure not due to bonding" is any other failure that rendered the device unsuitable for pressure testing. These failures include: inlet pin ejection, inlet seal rupture, or bulk PDMS splitting (see supplemental figure S4). Qualitatively, a bond failure and a "failure not due to bonding" are visually distinct and clearly distinguishable during experimental testing. All reported "failure not due to bonding" in figure 4 occurred at 60 PSI. The incidents of device failure demonstrate that at such high pressures (60 PSI), the bond strength of the layers is no longer the limiting operational constraint. In fact, 60 PSI is well above a practical operating pressure in multilayer microfluidics [1,22,30 REF https://doi.org/10.1002/(SICI)1522-2683(20000101)21:1%3C27::AID-ELPS27%3E3.0.CO;2-C]. For high-pressure device operation, such failure modes can be mitigated by using an epoxy resin or polymer sealant to irreversibly bond the inlet pins to the PDMS ports [REF: 10.1088/0960-1317/14/11/008 and http://stacks.iop.org/jm/11/577]. While such methods can withstand pressures higher than 60 PSI, these connections are irreversible, and the epoxy resin can contaminate inlet channels causing clogging and compromising biocompatibility.

The majority of devices fabricated in this study using the on-ratio protocol were able to withstand up to 60 PSI. In order for such a strong bond to exist, covalent interactions must exist across the bonding interface. Secondary forces between polymer chains are not sufficient for creating a strong, permanent bond [31]. To have covalent interactions across the bonding interface, polymer chains would have to bridge the bonding interface. Consequently, our results support the theory that: 1.) enough monomers and unused crosslinker exist at the surfaces of each layer (due to the partial cure) to form polymer chains across the bonding interface, and/or 2.) there is sufficient self-diffusion of polymer chains between two layers of PDMS of identical composition to create an autohesive bond that can withstand normal microfluidic operating pressures of up to 60 PSI.

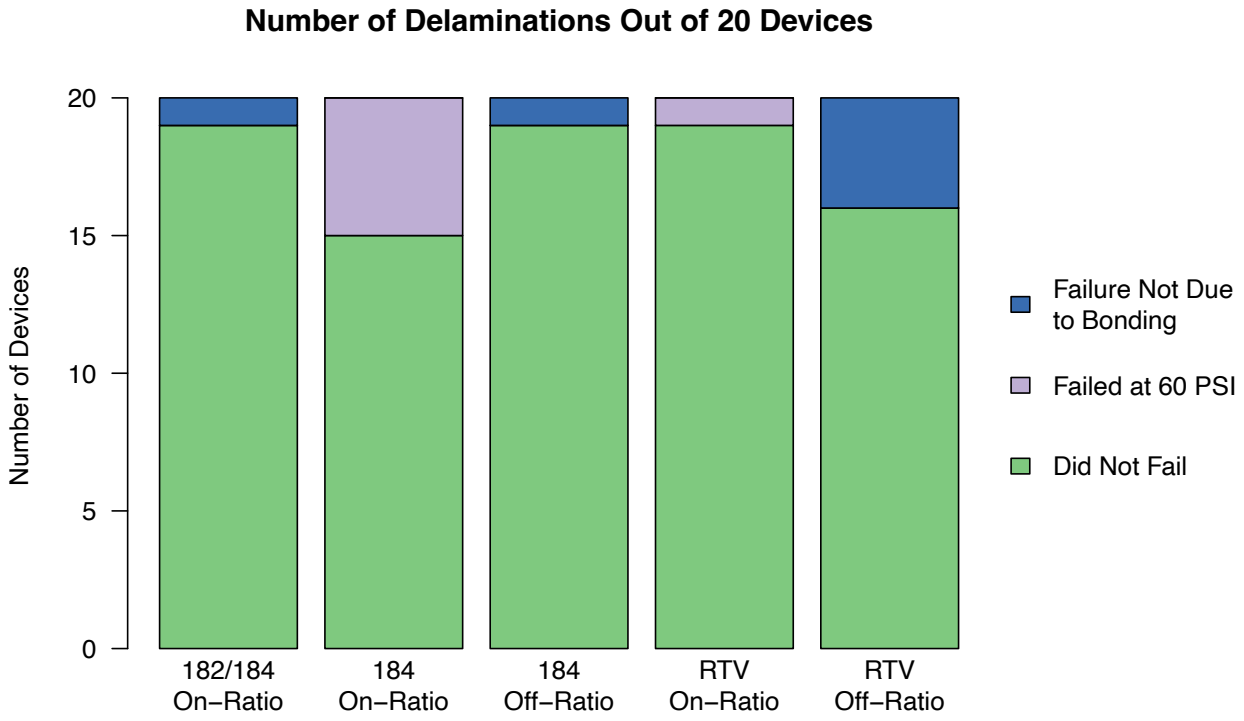

Figure 4. Results of bond performance. Pressurizing channels 150 μm wide and 25 μm tall resulted in no delamination at 30 and 45 PSI. At 60 PSI, 5/20 and 1/20 devices delaminated for 184 on-ratio and RTV on-ratio, respectively.

3.2 Burst Pressure Testing

To further test the limits of our bonding technique, pressure tests were performed on two variants: 182/184 on-ratio and 184 on-ratio, using large 7 mm diameter circular chambers. Despite the larger chambers, the majority of chips were able to withstand up to 45 PSI (figure 5). Standard microfluidic operating pressure is within the range of 20 - 45 PSI. This result demonstrates that even with extreme geometries, on-ratio bonding is effective for most microfluidic applications. From figure 5, we also see that the Sylgard 182/184 variant performs better than the Sylgard 184 variant. Again, we attribute this improved performance to Sylgard 182's longer cure time and thus facilitated partial curing. Interestingly, 182/184 had 1 more failure at 45 PSI than 184; this reveals a larger device-to-device variability for these pressure tests on large chambers. This correlates with observed variability with extreme aspect ratio pressure test [19].

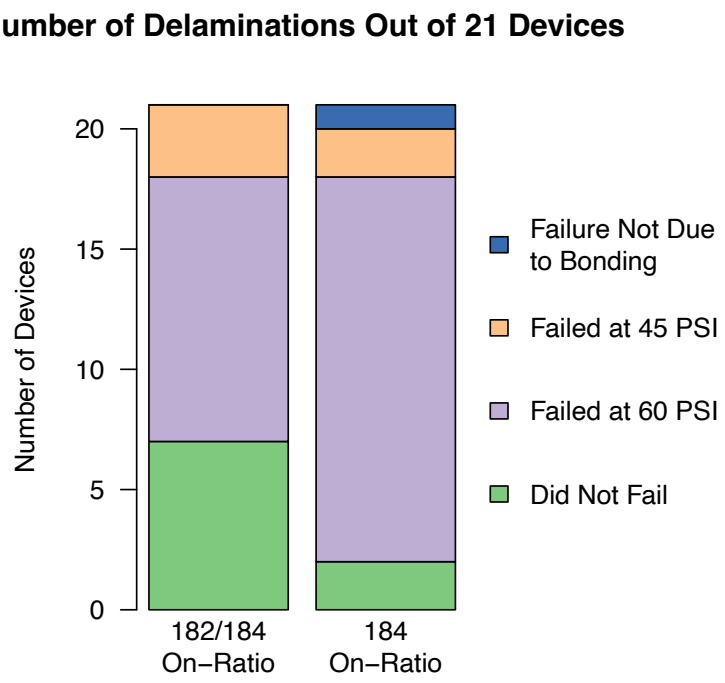

Figure 5. Large geometry bond performance: Chambers with a diameter of 7 mm were used to further verify the strength of on-ratio bonding. For both variants tested (182/184 on-ratio and 184 on-ratio), the majority of devices withstood up to 45 PSI. None of the devices failed at 30 PSI.

3.3 Baking Tolerances

When conducting repeated trials to determine the optimal partially cured baking time for on-ratio variants, we noticed that the range for a tolerable partial cure for on-ratio variants to be much narrower than that of off-ratio variants. As mentioned in the methods section 2.2.1, baking past this narrow partial cure window would result in an unsuccessful bond, while baking shorter would present issues with alignment and hole punching. Off-ratio ensures that at least one of the layers will be partially cured by controlling for the amount of crosslinker in a particular layer. Thus, it has a greater tolerance to longer baking times. It may be that off-ratio layers with base-to-crosslinker ratios below 10:1 (i.e. 20:1) will remain indefinitely in a state of partial cure past a threshold baking time. The same cannot be said for on-ratio. Consequently, baking time is a critical variable in achieving a successful bond with on-ratio bonding.

3.4 Valve Responsivity

From figure 6, the valve responsiveness of the 182/184 on-ratio devices had a closing time comparable to the 184 off-ratio devices, both averaging about 10 ms. For opening times, the 184 off-ratio devices performed over twice as fast; however, these differences are on the order of a few milliseconds and have negligible effect on typical operation of the devices.

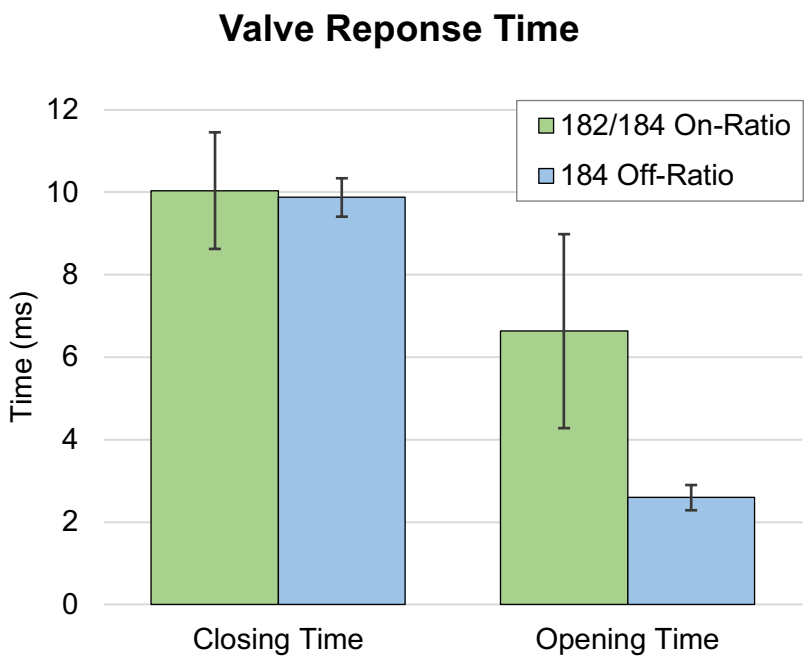

Figure 6. Comparison of Valve Opening and Closing Time: The 182/184 on-ratio devices had a closing time similar to that of the 184 off-ratio devices, with averages at 10.0 ms and 9.9 ms for the on-ratio devices and off-ratio devices, respectively. For opening times, the 184 off-ratio devices were over twice as fast than the 182/184 on-ratio devices, averaging 2.6 ms versus 6.6 ms for the 182/184 on-ratio devices. Error bars represent 2 standard errors

4. Conclusion

The use of on-ratio bonding provides an effective alternative to off-ratio bonding at a normal operating pressure range of 20 - 45 PSI (138 - 310 kPa). We showed that on-ratio bonding is robust and compatible with fabricating integrated elastomeric valves for two standard PDMS variants: Sylgard 184 and RTV 615. We also demonstrate improved on-ratio bond strength with a combination of Sylgard 184 and Sylgard 182 for the thick and thin layers respectively. When using Sylgard 182, we found no significant negative impact on valve responsivity. Furthermore, similar to off-ratio bonding, on-ratio bonding permits repeated manipulation of the layers during alignment before permanent bonding, a critical component of valve fabrication. We note that the most crucial step for successful on-ratio bonding is the partial curing, which requires careful optimization. Overall, this technique stands to contribute to lowering cost, improved material performance, and increased biocompatibility for multilayer soft-lithography [23,24].

Acknowledgements

We would like to thank Gabriel Dorlhiac for his assistance with measurements involving the scanning confocal microscope and spectrophotometer. We would also like to thank Paul Lum

whose discussion inspired this investigation. Finally, we would like to thank all members of the Streets Lab for their support. Research reported in this publication was supported by the University of California, Berkeley, Department of Bioengineering and the National Institute of General Medical Sciences of the National Institutes of Health [Grant Number R35GM124916]. Andre Lai is supported by the UC Berkeley Haas Scholars Program. Nicolas Altemose is a Howard Hughes Medical Institute Gilliam Fellow. Aaron Streets is a Chan Zuckerberg Investigator.

References

[1] Thorsen T, Maerkl S J and Quake S R 2002 Microfluidic large-scale integration *Science (80-.).* **298** 580–4

[2] Marcy Y, Ouverney C, Bik E M, Losekann T, Ivanova N, Martin H G, Szeto E, Platt D, Hugenholtz P, Relman D A and Quake S R 2007 Dissecting biological “dark matter” with single-cell genetic analysis of rare and uncultivated TM7 microbes from the human mouth *Proc. Natl. Acad. Sci.* **104** 11889–94

[3] Hansen C L, Sommer M O A and Quake S R 2004 Systematic investigation of protein phase behavior with a microfluidic formulator *Proc. Natl. Acad. Sci.* **101** 14431–6

[4] Rockel S, Geertz M and Maerkl S J 2012 MITOMI: A microfluidic platform for in vitro characterization of transcription factor-DNA interaction *Methods Mol. Biol.* **786** 97–114

[5] Liu J, Enzelberger M and Quake S 2002 A nanoliter rotary device for polymerase chain reaction *Electrophoresis* **23** 1531

[6] Ottesen E A, Jong W H, Quake S R and Leadbetter J R 2006 Microfluidic digital PCR enables multigene analysis of individual environmental bacteria *Science (80-.).* **314** 1464–7

[7] White A K, VanInsberghe M, Petriv O I, Hamidi M, Sikorski D, Marra M A, Piret J, Aparicio S and Hansen C L 2011 High-throughput microfluidic single-cell RT-qPCR *Proc. Natl. Acad. Sci.* **108** 13999–4004

[8] Kaestli A J, Junkin M and Tay S 2017 Integrated platform for cell culture and dynamic quantification of cell secretion *Lab Chip* **17** 4124–33

[9] Kim S, De Jonghe J, Kulesa A B, Feldman D, Vatanen T, Bhattacharyya R P, Berdy B, Gomez J, Nolan J, Epstein S and Blainey P C 2017 High-throughput automated microfluidic sample preparation for accurate microbial genomics *Nat. Commun.* **8** 13919

[10] Hansen C L, Skordalakes E, Berger J M and Quake S R 2002 A robust and scalable microfluidic metering method that allows protein crystal growth by free interface diffusion *Proc. Natl. Acad. Sci.* **99** 16531–6

[11] Marcus J S, Anderson W F and Quake S R 2006 Microfluidic single-cell mRNA isolation and analysis *Anal. Chem.* **78** 3084–9

[12] Streets A M, Zhang X, Cao C, Pang Y, Wu X, Xiong L, Yang L, Fu Y, Zhao L, Tang F and Huang Y 2014 Microfluidic single-cell whole-transcriptome sequencing *Proc. Natl. Acad. Sci.* **111** 7048–53

[13] Unger M A, Chou H P, Thorsen T, Scherer A and Quake S R 2000 Monolithic microfabricated valves and pumps by multilayer soft lithography. *Science* **288** 113–6

[14] Duffy D C, McDonald J C, Schueller O J A and Whitesides G M 1998 Rapid prototyping of microfluidic systems in poly(dimethylsiloxane) *Anal. Chem.* **70** 4974–84

[15] Satyanarayana S, Karnik R N and Majumdar A 2005 Stamp-and-stick room-temperature bonding technique for microdevices *J. Microelectromechanical Syst.* **14** 392–9

[16] Thompson S and Abate A R 2013 Adhesive-based bonding technique for PDMS

microfluidic devices3 *Lab Chip* **13** 632–5
[17] Haubert K, Drier T and Beebe D 2006 PDMS bonding by means of a portable, low-cost corona system *Lab Chip* **6** 1548
[18] Jeong O C, Yamamoto T, Lee S W, Fujii T and Konishi S 2005 Surface Modification, Mechanical Property, and Multi-Layer Bonding of PDMS and its Applications *9th Int. Conf. Miniturized Syst. Chem. Life Sci.* **1** 202–4
[19] Eddings M A, Johnson M A and Gale B K 2008 Determining the optimal PDMS-PDMS bonding technique for microfluidic devices *J. Micromechanics Microengineering* **18** 067001
[20] Khanafer K, Duprey A, Schlicht M and Berguer R 2009 Effects of strain rate, mixing ratio, and stress–strain definition on the mechanical behavior of the polydimethylsiloxane (PDMS) material as related to its biological applications *Biomed. Microdevices* **11** 503–8
[21] Wang Z, Volinsky A A and Gallant N D 2014 Crosslinking effect on polydimethylsiloxane elastic modulus measured by custom-built compression instrument *J. Appl. Polym. Sci.* **131**
[22] Fordyce P M, Diaz-Botia C A, Derisi J L and Gomez-Sjoberg R 2012 Systematic characterization of feature dimensions and closing pressures for microfluidic valves produced via photoresist reflow *Lab Chip* **12** 4287–95
[23] Regehr K J, Domenech M, Koepsel J T, Carver K C, Ellison-Zelski S J, Murphy W L, Schuler L A, Alarid E T and Beebe D J 2009 Biological implications of polydimethylsiloxane-based microfluidic cell culture *Lab Chip* **9** 2132–9
[24] Lee J N, Jiang X, Ryan D and Whitesides G M 2004 Compatibility of mammalian cells on surfaces of poly(dimethylsiloxane) *Langmuir* **20** 11684–91
[25] Lau A T H, Yip H M, Ng K C C, Cui X and Lam R H W 2014 Dynamics of microvalve operations in integrated microfluidics *Micromachines* **5** 50–65
[26] Lam R H W, Kim M-C and Thorsen T 2009 Culturing Aerobic and Anaerobic Bacteria and Mammalian Cells with a Microfluidic Differential Oxygenator *Anal. Chem.* **81** 5918–24
[27] McDonald J C and Whitesides G M 2002 Poly(dimethylsiloxane) as a material for fabricating microfluidic devices *Acc. Chem. Res.* **35** 491–9
[28] White J A and Streets A M 2017 Controller for microfluidic large-scale integration *HardwareX*
[29] Brower K, Puccinelli R R, Markin C J, Shimko T C, Longwell S A, Cruz B, Gomez-Sjoberg R and Fordyce P M 2018 An open-source, programmable pneumatic setup for operation and automated control of single- and multi-layer microfluidic devices *HardwareX* **3** 117–34
[30] Araci I E and Quake S R 2012 Microfluidic very large scale integration (mVLSI) with integrated micromechanical valves *Lab Chip* **12** 2803–6
[31] Awaja F 2016 Autohesion of polymers *Polymer (Guildf).* **97** 387–407